Original Article

MOLECULAR METABOLISM

Pharmacological blockade of the EP3 prostaglandin E_2 receptor in the setting of type 2 diabetes enhances β-cell proliferation and identity and relieves oxidative damage

Karin J. Bosma [1,2,11], Spencer R. Andrei [1,2,11], Liora S. Katz [3], Ashley A. Smith [4], Jennifer C. Dunn [1,2], Valerie F. Ricciardi [2], Marisol A. Ramirez [5,6], Sharon Baumel-Alterzon [3], William A. Pace [7], Darian T. Carroll [4], Emily M. Overway [4], Elysa M. Wolf [8], Michelle E. Kimple [9,10], Quanhu Sheng [5,6], Donald K. Scott [3], Richard M. Breyer [1,2], Maureen Gannon [1,2,4,*]

ABSTRACT

Objective: Type 2 diabetes is characterized by hyperglycemia and inflammation. Prostaglandin E_2, which signals through four G protein-coupled receptors (EP1-4), is a mediator of inflammation and is upregulated in diabetes. We have shown previously that EP3 receptor blockade promotes β-cell proliferation and survival in isolated mouse and human islets *ex vivo*. Here, we analyzed whether systemic EP3 blockade could enhance β-cell mass and identity in the setting of type 2 diabetes using mice with a spontaneous mutation in the leptin receptor ($Lepr^{db}$).

Methods: Four- or six-week-old, db/+, and db/db male mice were treated with an EP3 antagonist daily for two weeks. Pancreata were analyzed for α-cell and β-cell proliferation and β-cell mass. Islets were isolated for transcriptomic analysis. Selected gene expression changes were validated by immunolabeling of the pancreatic tissue sections.

Results: EP3 blockade increased β-cell mass in db/db mice through enhanced β-cell proliferation. Importantly, there were no effects on α-cell proliferation. EP3 blockade reversed the changes in islet gene expression associated with the db/db phenotype and restored the islet architecture. Expression of the GLP-1 receptor was slightly increased by EP3 antagonist treatment in db/db mice. In addition, the transcription factor nuclear factor E2-related factor 2 (Nrf2) and downstream targets were increased in islets from db/db mice in response to treatment with an EP3 antagonist. The markers of oxidative stress were decreased.

Conclusions: The current study suggests that EP3 blockade promotes β-cell mass expansion in db/db mice. The beneficial effects of EP3 blockade may be mediated through Nrf2, which has recently emerged as a key mediator in the protection against cellular oxidative damage.

Keywords Type 2 diabetes; Mouse model; Prostaglandin E_2; Beta cell proliferation; Nrf2

1. INTRODUCTION

Type 2 diabetes (T2D) results from the failure of insulin-secreting β cells to compensate for elevated metabolic demand, thereby resulting in diminished expansion of functional β-cell mass [1,2]. G-protein-coupled receptors (GPCRs) expressed in islets play a role in β-cell function and/or regulation of β-cell mass [3]. One GPCR currently targeted as a T2D therapy is the glucagon-like peptide 1 (GLP-1) receptor (GLP-1R), which couples with stimulatory G proteins (G_S). In mice, exogenous GLP-1 treatment increases glucose-stimulated insulin secretion (GSIS), β-cell proliferation, and β-cell survival [4]. Although GLP-1-based therapies have been successful in many cases, they are not effective in all individuals with T2D [5]. The increased activity of GPCRs that couple with inhibitory G proteins (G_i) in some individuals may provide an explanation for these variable responses to GLP-1-based treatments.

The chronic hyperglycemia and systemic inflammation observed in T2D are associated with increased levels of circulating prostaglandin

[1]Dept. of Veterans Affairs Tennessee Valley Authority, Nashville, TN, USA [2]Dept. of Medicine, Vanderbilt University Medical Center, Nashville, TN, USA [3]Diabetes, Obesity and Metabolism Institute, Icahn School of Medicine at Mount Sinai, New York, NY, USA [4]Dept. of Molecular Physiology and Biophysics, Vanderbilt University, Nashville, TN, USA [5]Center for Quantitative Sciences, Vanderbilt University Medical Center, Nashville, TN, USA [6]Dept. of Biostatistics, Vanderbilt University Medical Center, Nashville, TN, USA [7]Dept. of Biomedical Engineering, Vanderbilt University, Nashville, TN, USA [8]Program in Cancer Biology, Vanderbilt University, Nashville, TN, USA [9]Dept. of Medicine, University of Wisconsin, Madison, WI, USA [10]William S. Middleton Memorial Veterans Hospital, Madison, WI, USA

[11] Karin J. Bosma and Spencer R. Andrei contributed equally to this work.

*Corresponding author. Dept. of Medicine, Div. of Diabetes, Endocrinology, and Metabolism, Vanderbilt University Medical Center, 2213 Garland Ave., 7465 MRB IV, Nashville, TN 37232-0475, USA. Fax: +615 936 1667. E-mail: Maureen.gannon@vumc.org (M. Gannon).

Received July 8, 2021 • Revision received September 2, 2021 • Accepted September 23, 2021 • Available online 6 October 2021

https://doi.org/10.1016/j.molmet.2021.101347

E_2 (PGE_2; 6, 7), which has been implicated in β-cell dysfunction and loss of β-cell identity [7—15]. Downstream effects of PGE_2 signaling are carried out by the E-prostanoid (EP) receptors, EP1-4. The expression of EP3, a G_i-coupled receptor, is increased in islets from humans with T2D and mouse models of T2D [7,16]. Both EP3 and EP4, a G_s-coupled receptor, have emerged as potential therapeutic targets for modulating β-cell mass dynamics and function. Recently, our lab demonstrated that pharmacological EP3 blockade promotes β-cell proliferation and survival in *ex vivo* mouse and human islets [16]; activation of EP4 enhanced β-cell survival in both mouse and human islets but stimulated β-cell proliferation only in human islets. Our group has shown that the downstream effectors that block EP3 and/or activate EP4 in β cells include PLCγ-1 and/or cAMP/PKA pathways, respectively [7,16]. Although the modulation of EP3 and EP4 activity has been shown to be beneficial in the context of mouse models of diabetes, the mechanisms for these effects were not analyzed. In particular, whether *in vivo* PGE_2 receptor modulation in the setting of T2D alters β-cell mass dynamics or preserves β-cell identity has not been determined.

The current study explores whether *in vivo* pharmacological antagonism of EP3 enhances β-cell proliferation and mass in the setting of T2D using the db/db mouse model, which contains a spontaneous mutation in the leptin receptor, resulting in hyperphagia, obesity, and hyperglycemia. Given our previous studies using isolated mouse and human islets *ex vivo*, we predicted that *in vivo* EP3 blockade would enhance β-cell proliferation and survival, which would ultimately result in β-cell mass expansion. We found that systemic blockade of EP3 enhanced β-cell proliferation and mass in db/db mice, with no effect on α-cell proliferation. Whole transcriptome analysis at the onset of diabetes revealed distinct gene expression changes in db/db mice compared with controls. EP3 blockade reversed the db/db islet phenotype, including changes in the islet architecture and the expression of some β-cell identity genes. GLP-1R protein, absent in db/db islets, was partially restored by treatment with the EP3 antagonist. EP3 blockade also increased the expression of the transcription factor nuclear factor E2-related factor 2 (Nrf2) and some of its downstream targets in islets from db/db mice. As Nrf2 has recently emerged as a key mediator in the protection against cellular oxidative damage [17—19], our results provide strong support for PGE_2 signaling modulating β-cell redox state and subsequently β-cell identity and function.

2. MATERIALS AND METHODS

2.1. Animal models

Lepr$^{db/+}$ (db/+) C57BL/6J (Jax #000697) mice were purchased from the Jackson Laboratory (Bar Harbor, ME), and *Lepr*$^{db/db}$ (db/db) mice were bred in-house. Mice were housed in a controlled-temperature environment with a 12-hr light cycle and *ad libitum* access to food (11% kcal from fat; 5LJ5, Purina, St. Louis, MO) and water except when otherwise noted. Four- or six-week-old male mice were injected daily for two weeks with either 20 mg/kg DG-041 or volume-matched vehicle (phosphate buffered saline (PBS) + 10% dimethyl sulfoxide (DMSO)) subcutaneously. Body weights were assessed daily to ensure that the mice did not lose more than 20% body weight. Mice were euthanized at six or eight weeks of age. All mice were maintained on a C57BL/6J background and handled in accordance with the Guide for the Care and Use of Laboratory Animals (NIH). Mice were housed in the Vanderbilt University Medical Center (Nashville, TN) animal care facility, which is accredited by the American Association for Accreditation of Laboratory Animal Care. All mouse experiments were approved by the Institutional Animal Care and Use Committee of Vanderbilt University Medical Center.

2.2. Mouse pancreas immunolabeling

Pancreata were dissected, weighed, and fixed for four hours in 4% paraformaldehyde and subsequently dehydrated in an ethanol series before paraffin embedding. Sections were rehydrated and subjected to sodium-citrate-induced antigen retrieval. The primary antibodies used were: guinea pig anti-insulin (1:400; Dako #A0564, Carpinteria, CA), mouse anti-glucagon (1:500; EMD Millipore #MABN238, Bellerica, MA), rabbit anti-Ki67 (1:500; Abcam #ab15580, Cambridge, MA), rabbit anti-GLP-1R (1:500; Abcam #ab218532, validated on *Glp1*−/− tissue in [20]), or mouse anti-GLP-1R (1:30, DHSB mAb #7F38, validated on *Glp1*−/− tissue in [21]). Apoptosis was detected using an ApoAlert terminal deoxynucleotidyl transferase dUTP nick end labeling (TUNEL) assay kit according to the manufacturer's instructions (Clontech, Mountain View, CA). The primary antibodies were detected with the appropriate species-specific secondary antibodies (Jackson ImmunoResearch Laboratories, West Grove, PA): Cy2-conjugated anti-guinea pig IgG (1:400; #GP 706-225-148), Cy3-conjugated anti-rabbit IgG (1:400; #Rb 711-165-152), and Cy5-conjugated anti-mouse IgG (1:400; #715-175-151). Nuclei were visualized with 40,60-diamidino-2-phenylindole (DAPI, 1 μg/mL for 2 min; Molecular Probes D1306, Eugene, OR). Images were acquired with a ScanScope FL slide scanner (Aperio Technologies, Vista, CA) and quantified using MetaMorph 6.1 (Molecular Devices, Sunnyvale, CA). Positive staining was determined by double-blinded, manual quantification and cross-checked using macros generated with the CytoNuclearFL algorithm in eSlide Manager (Aperio Technologies, Vista, CA). A minimum of 3,000 β cells were counted for β-cell proliferation, death, and α:β ratio. Data are represented as Ki67-, TUNEL-, or glucagon-positive cells relative to the entire insulin+ and/or glucagon+ population. The primary antibodies used for Nrf2 validation and 8-hydroxy-2-deoxyguanosine (8OHdG) immunolabeling included: guinea pig insulin (1:1000; Dako #A0564, Carpinteria, CA), mouse glucagon (1:1000, Abcam #ab10988 with Nrf2 or 1:700, Abcam #ab63623 with 8OHdG), and either rabbit Nrf2 (Cayman Chemicals #10214 at 1:250, Ann Arbor, MI) or mouse 8OHdG (Abcam #ab62623 at 1:100). The primary antibodies were detected with the appropriate species-specific secondary antibodies: Alexa488-conjugated anti-mouse IgG (Invitrogen #A11029), Alexa594-conjugated anti-rabbit IgG (Invitrogen #A11037), or Alexa647-conjugated anti-guinea pig IgG (Invitrogen #A21450) Nuclei were stained with DAPI. Cells were imaged with a Zeiss Axioplan 2 microscope or an Olympus DP74 microscope with cellSens Standard software version 2. For the quantification of nuclear Nrf2 and 8OHdG, 250—800 insulin-positive cells per mouse were counted, and the percentage of the cells was calculated with nuclear labeling for Nrf2 or 8OHdG.

2.3. β-cell mass quantification

Sections were cut serially at 5 μm and placed on slides pre-treated with Sta-On (Leica Biosystems, Lincolnshire, IL). Six to seven slides per animal (separated by at least 250 μm and sampling the entire pancreas) were immunolabeled for insulin, visualized *via* the DAB Peroxidase Substrate Kit (Vector Laboratories, Burlingame, CA), and counterstained with eosin. Quantification of β-cell mass was calculated as described previously [22]. In brief, one pancreatic section per slide was scanned using a ScanScope CS scanner, and the images were processed identically with the ImageScope software (Aperio Technologies, Vista, CA). β-cell mass was measured by determining the ratio of insulin + area to the total pancreatic area of

all the scanned sections per animal multiplied by the wet weight of the pancreas.

2.4. Islet isolations

Following euthanasia, the pancreata were perfused with 0.5 mg/mL type IV collagenase dissolved in Hanks Balanced Salt Solution (HBSS) containing Ca^{2+} and Mg^{2+}, as described previously [23]. After digestion at 37°C, lysates were washed and resuspended in RPMI 1640 containing 5.6 mM glucose and 10% fetal bovine serum. The islets were handpicked and prepared for RNA isolation or static incubation assays.

2.5. Static incubation assays

Handpicked islets were allowed to recover in RPMI without FBS overnight, as described previously [23]. The islets were washed with Krebs solution containing the following (mM): 2.8 glucose, 102 NaCl, 5 KCl, 1.2 $MgCl_2$, 2.7 $CaCl_2$, 20 HEPES, 5 $NaHCO_3$, and 10 mg/mL BSA (pH 7.4). They were incubated at 37°C for 45 min and roughly 10 islet equivalents were transferred into the wells of a 12-well plate containing 1 mL pre-warmed KRB solution. GSIS was measured by calculating the total percentage of insulin secreted within a 45-minute treatment duration. Technical replicates were conducted for each experiment. Insulin ELISA kits (ALPCO, Salem, NH) were used to measure the insulin secretion, as per the manufacturer's instructions.

2.6. Intraperitoneal glucose tolerance tests (IP-GTT)

For IP-GTT, the mice were fasted overnight. Glucose (2 mg/kg) was injected intraperitoneally. Blood glucose was measured *via* the tail vein (2 μL) at 0, 15, 30, 60, 90, and 120 min following injections using an Accu-check glucometer and glucose strips (Roche, Indianapolis, IN). Statistical analyses were performed on the area under the curve (AUC) to the baseline.

2.7. RNA isolation and sequencing

Pancreatic islets from vehicle- or DG-041-treated db/+ or db/db mice were isolated and prepared for RNA extraction in 1 ml Trizol reagent (ThermoFisher, Waltham, MA). RNA was isolated using the RNeasy Mini Kit (Qiagen, Germantown, MD) according to the manufacturer's instructions. The RNA concentration and integrity were assessed using a ND-1000 spectrophotometer (NanoDrop) and the 2100 Electrophoresis Bioanalyzer (Agilent, Santa Clara, CA) at the Vanderbilt Technologies for Advanced Genomics (VANTAGE) Core. Libraries of 150 bp fragments were generated for each sample by the VANTAGE Core. Libraries were pair-end sequenced to a depth of 50 million reads by Illumina HiSeq (San Diego, CA).

2.8. Statistics

Student's *t*-test, one- or two-way ANOVA, and the Bonferroni *post hoc* test were performed where appropriate (and as indicated in each respective figure legend). The statistical significance was set at $p < 0.05$ (one symbol), $p < 0.01$ (two symbols), and $p < 0.001$ (three symbols). All results are expressed as mean ± SEM. Statistical analysis was conducted using Prism 8.0 (GraphPad software). For RNA-Seq analysis, the reads were trimmed to remove the adapter sequences using Cutadapt v2.5 [24] and aligned to the GENCODE GRCm38.p6 genome using STAR v2.7.2b [25]. GENCODE vM24 gene annotations were provided to STAR to improve the accuracy of mapping. Quality control on both raw reads and adaptor-trimmed reads was performed using FastQC v0.11.8 (www.bioinformatics.babraham.ac.uk/projects/fastqc). FeatureCounts v1.6.4 [26] was used to count the number of mapped reads to each gene. Significantly differentially expressed genes with an FDR-adjusted *p*-value <0.05 and absolute fold change >2.0 were detected by DESeq2 (v1.24.0) [27]. Heatmap3 [28] was used for cluster analysis and visualization. Gene ontology and KEGG pathway overrepresentation analyses were performed on differentially expressed genes using the WebGestaltR package [29]. One of the vehicle-treated db/+ samples was statistically determined to be an outlier and was thus eliminated from further analysis.

3. RESULTS

3.1. EP3 antagonist treatment promotes β-cell mass expansion in pre-diabetic db/db mice

Mice homozygous for a spontaneous mutation in the leptin receptor (db/db) show elevations in blood glucose between four to eight weeks of age. To determine whether EP3 blockade *in vivo* has beneficial effects on β-cell mass in the setting of T2D, we treated db/db mice with the EP3 antagonist DG-041. As a guideline, we referred to the study by Guo et al. (2013), which identified a critical time window of increased β-cell proliferation and β-cell compensation between four and six weeks of age in db/db mice [30]. After this time point, β-cell proliferation declines and β-cell mass decreases, leading to overt diabetes. We thus utilized two different injection protocols: four to six weeks of age or six to eight weeks of age to determine whether modulation of EP3 receptor activity could enhance or extend β-cell compensation. DG-041 (20 mg/kg) or vehicle was subcutaneously administered daily for two weeks beginning at four or six weeks of age to db/+ and db/db male mice; this dose was chosen based on published data demonstrating effective blockade of EP3 with minimal off-target effects [31]. Pancreata were collected at six or eight weeks of age and immunolabeled for insulin to quantify β-cell mass. EP3 blockade resulted in a significant, more than two-fold increase in β-cell mass only in db/db mice treated with DG-041 from six to eight weeks of age (vehicle: 1.11 mg ± 0.16; DG-041: 2.62 mg ± 0.35; $p < 0.05$; Figure 1). Notably, DG-041 treatment had no significant effect on β-cell mass in db/+ mice at either time point.

To understand the mechanism underlying β-cell mass expansion in response to EP3 antagonist, we analyzed β-cell proliferation and survival. Although we did not observe an effect on β-cell proliferation in db/db mice treated with DG-041 from six to eight weeks of age, an increase in β-cell proliferation was observed in mice treated from four to six weeks (as indicated by Ki67 labeling) compared with vehicle-treated animals (Figure 2). Systemic EP3 blockade had no significant effect on β-cell replication in db/+ mice at either time point. Importantly, in agreement with our *ex vivo* studies [16], EP3 blockade did not increase α-cell proliferation in any genotype at either time point (data not shown). Despite the beneficial effects of EP3 blockade on β-cell survival in human and mouse islets *ex vivo* [16], we did not observe a significant difference in TUNEL labeling across any treatment group within the respective cohorts after two weeks of DG-041 treatment at either time point (Supplemental Figure 1).

3.2. In vivo EP3 blockade does not alter insulin secretion in isolated islets from db/db mice

A previous study from our group demonstrated that *ex vivo* treatment of islets with the polyunsaturated fatty acid, eicosapentaenoic acid, enhanced β-cell function concomitant with reductions in *Ptger3*/EP3 expression [6]. However, our group has also reported that islets isolated from eight-week-old global EP3 KO mice do not display differences in GSIS when compared with their control counterparts [32]. In addition, EP3 KO mice fed a HFD do not show altered GSIS when compared with chow-fed mice at approximately 30 weeks of age [32].

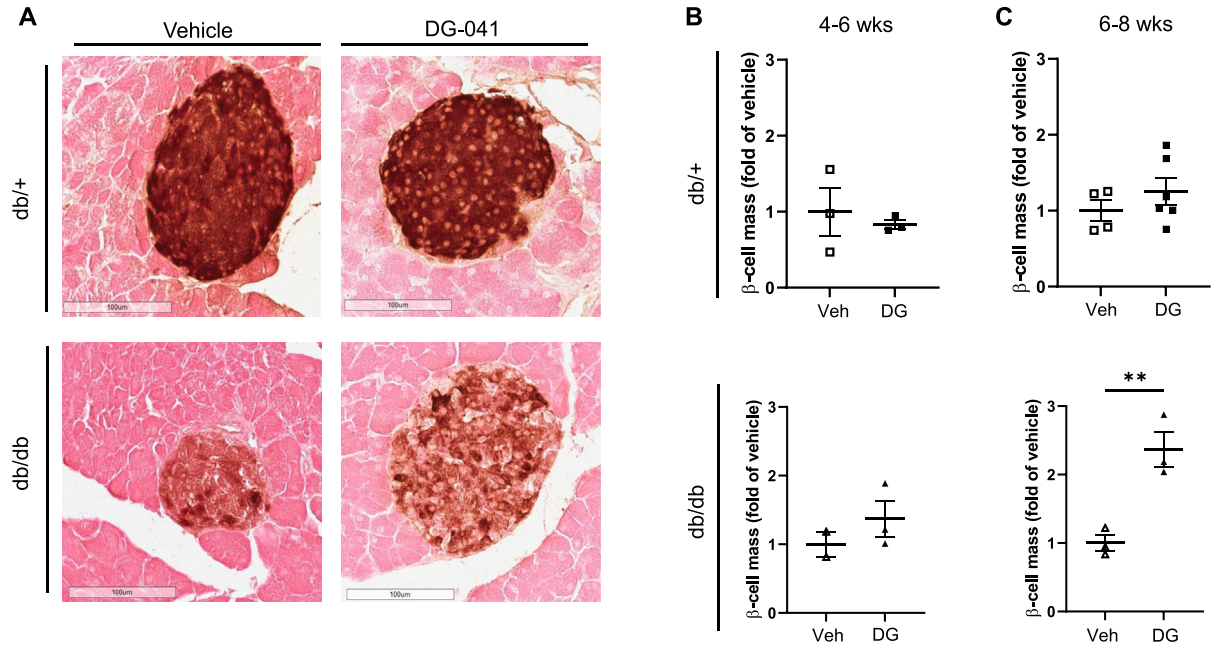

Figure 1: Systemic EP3 blockade promotes β-cell mass expansion in db/db mice. (A) Representative images of insulin-labeled (brown) pancreatic sections from vehicle (veh)- or DG-041 (DG)-treated db/+ and db/db mice treated from 6 to 8 weeks of age. (B) β-cell mass from 4 to 6 weeks of age and (C) 6–8 weeks of age. Empty squares, db/+ veh. Filled squares, db/+ DG. Empty triangles, db/db veh. Filled triangles, db/db DG. *versus vehicle. Two asterisks indicate $p < 0.01$. Data were analyzed using Student's *t*-test and Bonferroni *post hoc* analysis. (Scale bar, 100 μm)

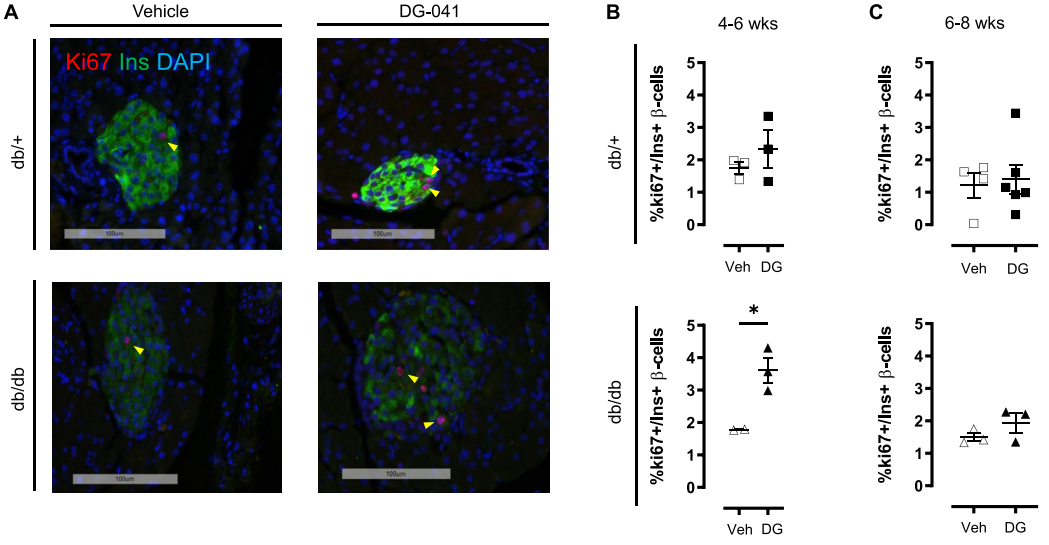

Figure 2: β-cell proliferation is increased in db/db mice in response to EP3 blockade. (A) Representative images of pancreatic sections obtained from vehicle (veh)- or DG-041 (DG)-treated db/+ or db/db mice treated from 4 to 6 weeks of age and immunolabelled for Ki67 (red) and insulin (green) and stained with DAPI (blue). β-cell proliferation was quantified by the percentage of Ki67-expressing insulin+ cells. (B) Summarized data for vehicle- and DG-treated db/+ or db/db mice treated from 4 to 6 weeks of age. (C) Summarized data for vehicle- and DG-treated db/+ or db/db mice treated from 6 to 8 weeks of age. Yellow arrows indicate Ki67/insulin dual-positive cells. Empty squares, db/+ veh. Filled squares, db/+ DG. Empty triangles, db/db veh. Filled triangles, db/db DG. Data were analyzed using Student's *t*-test and Bonferroni *post hoc analysis*. (Scale bar, 100 μm)

In the current study, insulin secretion in static incubation assays from islets isolated from db/+ or db/db mice was not significantly altered by *in vivo* EP3 blockade when examined at either low or high glucose concentrations (Supplemental Figure 2). The current DG-041 treatment protocol had no effect on insulin sensitivity (data not shown) or glucose tolerance in db/+ or db/db mice (Supplemental Figure 3). Since the global inactivation of *Ptger3* resulted in increased hepatic lipid content and increased fat mass, we examined this in the DG-041-treated mice. Two weeks of EP3 antagonist treatment did not increase the hepatic lipid content over the db/db genotype alone (data not shown). However,

we did observe a slight, but significant increase in epididymal fat pad mass only in the DG-041-treated db/db mice compared with vehicle-treated mice (Supplemental Figure 4).

3.3. Transcriptomic analysis reveals changes in gene expression in db/db mice at diabetes onset

To begin to understand the mechanisms whereby EP3 blockade enhances β-cell mass dynamics, we performed transcriptomic analysis on whole islets isolated from eight-week-old db/+ or db/db mice treated with or without DG-041 for two weeks. We observed modest variability in gene expression between the biological replicates of each genotype (Figure 3A). Comparisons between the data sets revealed distinct patterns of differentially expressed (DE) genes, in particular between islets from db/+ and db/db mice regardless of the EP3 antagonist treatment, with fewer DE genes between untreated and treated mice within a given genotype. (Supplemental Figure 5A).

We identified 2,986 DE genes between the vehicle-treated db/+ and db/db groups, including 42 key islet genes that were altered in db/db islets compared with db/+ islets (Figure 3B). For example, several transcription factors involved in β-cell identity and maturity (*Mafa, Nkx2.2, Nkx6.1, Pdx1*) were downregulated. Other genes involved in β-cell function that were downregulated in islets from db/db include *Ins1, Gck, Slc2a2,* and *Ucn3*, while glucagon (*Gcg*) and *Cck* were upregulated. Several key mediators of the insulin secretion pathway (*Kcnj11, Vamp2, Slc30a8, G6pc2*) were also downregulated in islets obtained from db/db mice (Figure 3B), mirroring a previous proteomic analysis of db/db islets at 12 weeks of age [33]. The expression of *Glp1r* was also downregulated in db/db islets compared with db/+ islets (Figure 3B). Other upregulated genes included transcription factors associated with immature endocrine cells (*Oc1, Mafb*) (Figure 3B) and several β-cell disallowed genes, including *Ldha, Aldob,* and *Aldh1a3*. *Ptger3,* the gene encoding EP3, was also upregulated in db/db mice compared with db/+mice (Figure 3B), as was *Ptger4,* which encodes the EP4 receptor.

3.4. EP3 antagonist treatment restores aspects of gene expression and islet architecture

Treatment with the EP3 antagonist DG-041 resulted in changes in the expression of key islet genes in islets from both db/+ mice (Figure 3C) and db/db mice (Figure 3D). Gene ontology analysis revealed that many DE genes were involved in signaling and communication, extracellular matrix, and protein binding (Supplemental Figure 5B). Only 17 genes were significantly DE in the islets from DG-041-treated db/db mice compared with vehicle-treated db/db mice (Supplemental Figure 5D). Of these 17 DE genes, most were upregulated including oxidoreductases involved in xenobiotic metabolism (*Cyp2e1, Cyp3a13*), while genes involved in extracellular matrix accumulation were downregulated (e.g. *Col10a1*). This supports previous studies implicating the role of EP3 in the regulation of extracellular matrix protein accumulation [34].

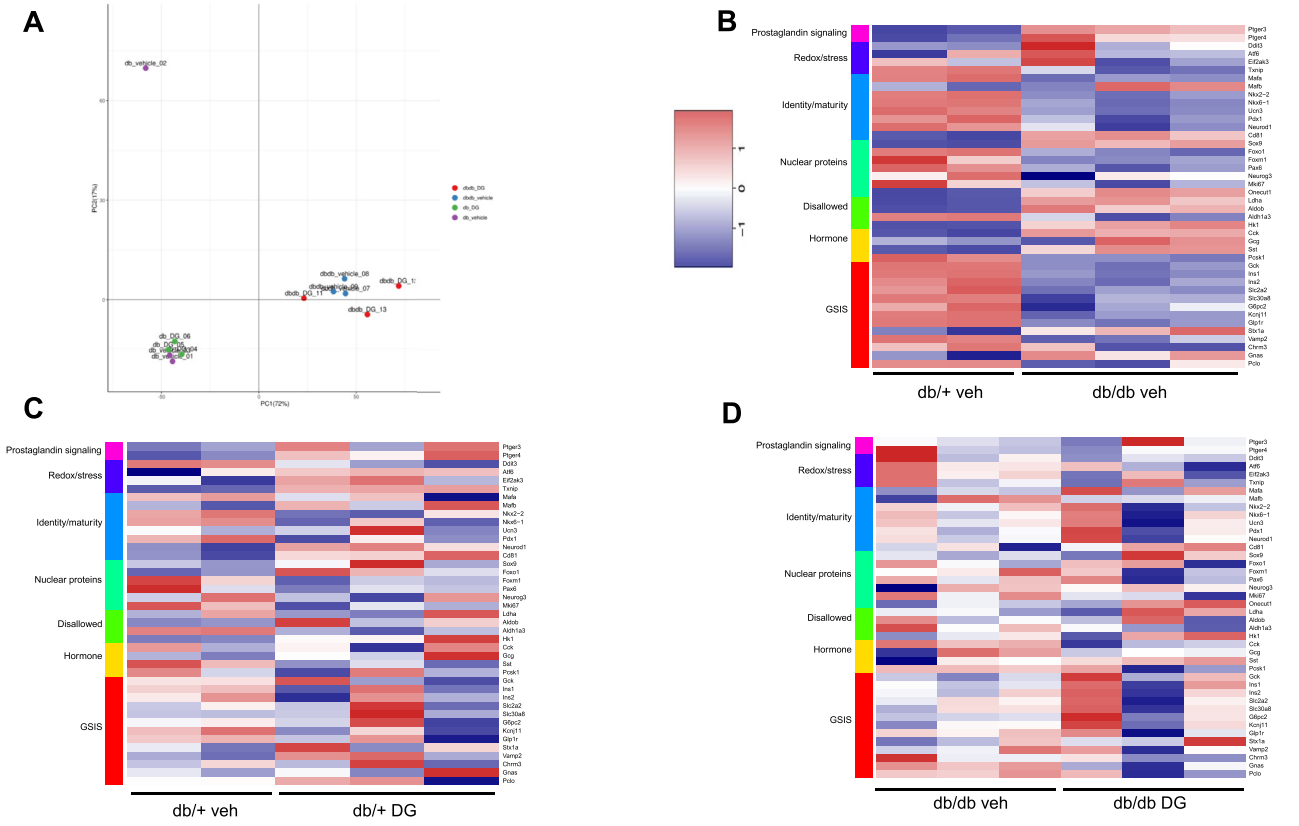

Figure 3: Genotype-dependent changes in gene expression in db/+ and db/db mice. (A) Principal component analysis based on gene expression from RNA sequencing for each of three biologic replicates for vehicle- or DG-041-treated db/+ or db/db mouse islets. Mice were treated from 6 to 8 weeks of age. db/+ veh2 was determined to be an outlier and was removed from further analysis. (B) Heatmap depicting alterations in the expression of 42 selected islet markers in vehicle-treated db/+ or db/db mouse islets. (C) Heatmap depicting alterations in the expression of 42 selected islet markers in vehicle-treated or DG-041-treated db/+ mouse islets. (D) Heatmap depicting alterations in the expression of 42 selected islet markers in vehicle-treated or DG-041-treated db/db mouse islets. For all heatmaps, red indicates high expression and blue indicates low expression. Samples are grouped by genotype or treatment.

In islets from db/db mice treated with DG-041, there was also an upregulation of genes correlated with β-cell identity (*Mafa, Nkx6.1*), β-cell function (*Ins1, Gck*), and insulin secretion (Figure 3D). Treatment with the EP3 antagonist reversed many of the gene expression changes observed in db/db islets (Figure 3D). Of note, the *Mki67* expression was decreased in six-to eight-week-old db/db mice treated with DG-041, which supports the immunolabeling data showing no increase in Ki67 labeling at this time point (Figure 2C).

Comparison between vehicle- and DG-041-treated db/db mouse islets revealed an overlap with several key cell adhesion genes that were upregulated in db/db mice compared with db/+ mice (*Madcam1, Tgfbi*), whereas others were downregulated (*Hapln4, Tenm4*) (Figure 4A), suggesting differences in cell—cell and cell—extracellular matrix interactions in db/db islets. Other DE genes encoding for proteins involved in cell—cell interactions and cell—matrix interactions such as collagens, integrins, and Eph receptors that were upregulated in db/db islets compared with db/+ islets were not affected significantly by treatment with the EP3 antagonist (Figure 4B).

When compared with their db/+ counterparts at eight weeks of age, we found that vehicle-treated db/db mice displayed reduced β/α-cell ratios (Figure 4C). At this age, db/db mice also have a "mixed islet" phenotype, where the normal islet architecture is disrupted, with α cells infiltrating the islet core [35,36] (Figure 4D). This phenotype is likely the result of the migration of the existing α cells located on the mantle into the core of the islet, although islet cell transdifferentiation cannot be ruled out at this time [37,38]. Treatment with the EP3 antagonist significantly improved the β/α-cell ratio in db/db mice (Figure 4C) and even more dramatically restored the islet architecture (Figure 4D).

Glp1r mRNA was dramatically decreased in db/db islets compared with db/+ islets, but restoration of gene expression was variable with EP3 blockade. To determine whether there was more of an effect on GLP-1R protein expression, we examined GLP-1R protein levels using immunolabeling with two different antibodies previously validated on tissue from GLP-1R knockout mice (Figure 5 and Supplemental Figure 6). GLP-1R protein was undetectable in db/db islets from untreated mice. Treatment with the EP3 antagonist partially restored GLP-1R, increasing its expression on the surface of a sub-population of

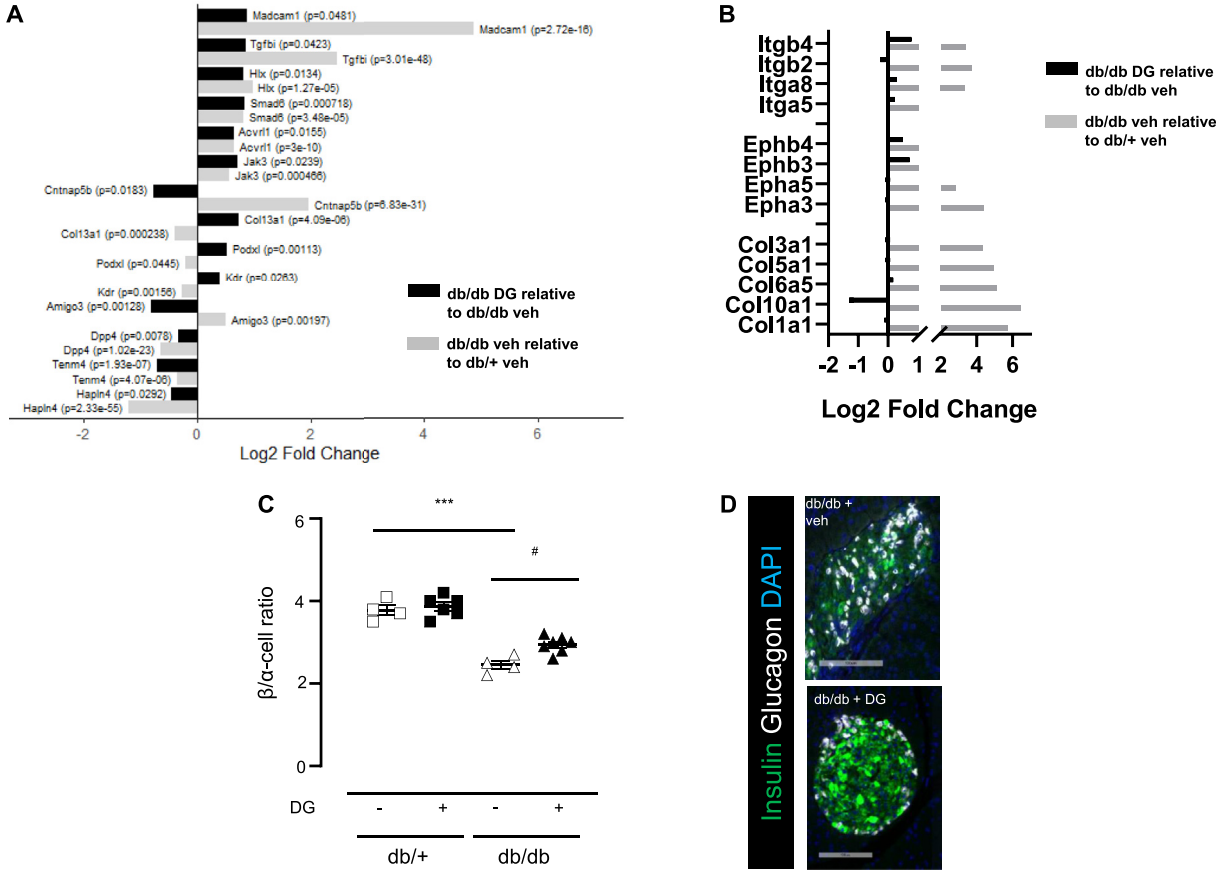

Figure 4: Effects of EP3 blockade on gene expression and islet architecture in db/db mice. (A) Gene ontology analysis of cell adhesion genes differentially expressed in DG-041-treated vs vehicle-treated db/db mice (black bars) and db/db vehicle vs db/+ vehicle (gray bars). The log2 fold change is plotted along the *x*-axis. (B) Summary of select differentially expressed collagen (Col), ephrin (Eph), and integrin (Itg) genes in DG-041-treated vs vehicle-treated db/db mice (black bars) and db/db vehicle vs db/+ vehicle (gray bars). The log2 fold change is plotted along the *x*-axis. (C) β/α-cell ratio in vehicle (−)- or DG-041 (+)-treated db/+ and db/db mice. β/α-cell ratio was determined by quantifying the total insulin + cells divided by the total glucagon + cells. Each point represents one mouse. (D) Representative images of the pancreatic sections showing the distribution of insulin+ (green) and glucagon+ (white) cells in db/db mice with and without DG-041 treatment. DAPI (blue). Empty squares, db/+ veh. Filled squares, db/+ DG-041. Empty triangles, db/db veh. Filled triangles, db/db DG-041. *versus veh-treated db/+, #versus veh-treated db/db. One symbol indicates $p < 0.05$; three symbols indicate $p < 0.001$. Mice were treated from 6 to 8 weeks of age for 14 days. All summarized data were analyzed using ANOVA or Student's *t*-test and Bonferroni *post hoc analysis*. (Scale bar, 100 μm).

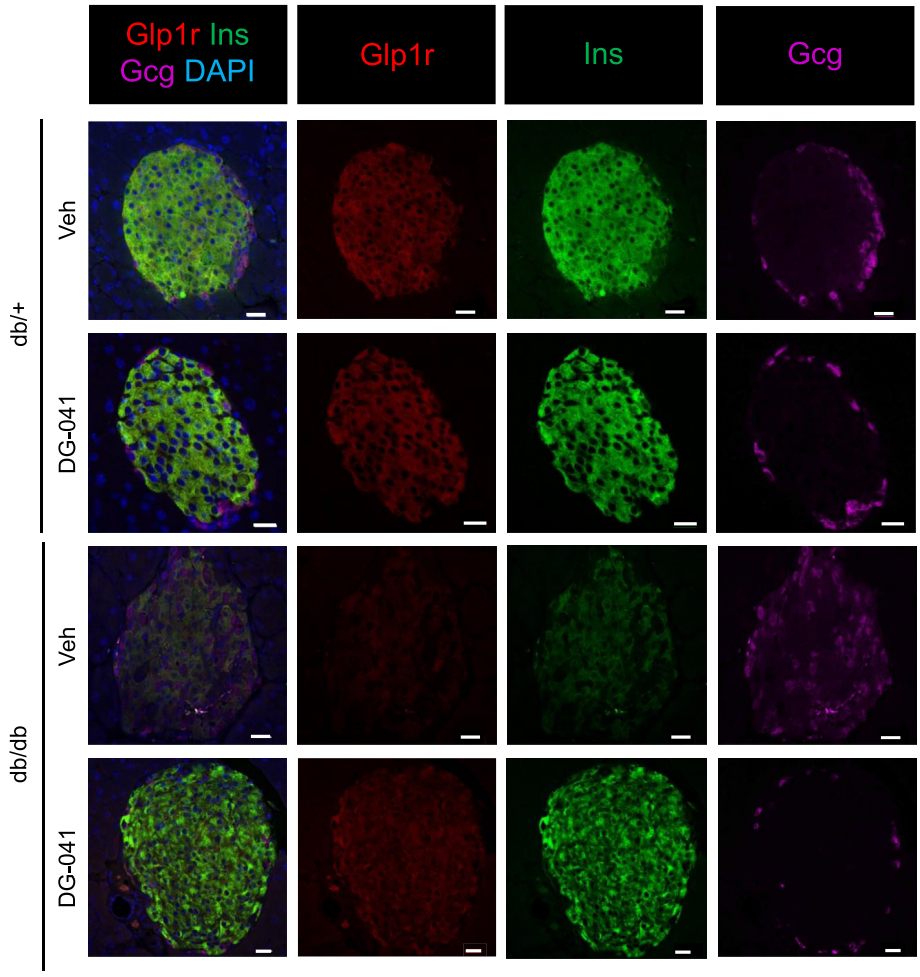

Figure 5: Effects of EP3 blockade on GLP-1R protein expression in db/+ and db/db mice. Paraffin-embedded sections from pancreata isolated from the indicated genotype and treatment groups were immunolabeled with antibodies directed against insulin (Ins; green), glucagon (Gcg; purple), or GLP-1R (Glp-1r; red). Nuclei were stained with DAPI (blue). Mice were treated from 6 to 8 weeks of age for 14 days. (Scale bar, 20 μm)

β-cells. EP3 blockade had no effect on GLP-1R protein in db/+ mice (Figure 5 and Supplemental Figure 6). In addition, we noticed a consistent increase in insulin protein immunolabeling with EP3 antagonist treatment in db/db mice (Figures 5–7).

3.5. EP3 blockade activates the Nrf2 antioxidant pathway

Nfe2l2, the gene encoding Nrf2, was upregulated in response to DG-041 treatment in db/db mice compared with db/+ mice (1.9-fold, adjusted *p*-value = 1.83E-07; Figure 6B). Nrf2 is a master transcriptional regulator of cellular antioxidant responses and plays an important role in promoting β-cell survival and proliferation [19,39,40]. Moreover, Nrf2 is activated by the prostaglandin signaling pathway [41–43], as well as the cAMP signaling pathway *via* GLP-1R [44]. Therefore, to assess whether Nrf2 induction might mediate the beneficial effects of DG-041, we performed immunolabeling of mouse pancreatic sections with insulin, glucagon, and Nrf2 antibodies. EP3 blockade increased the overall Nrf2 protein signal in db/+ and db/db mice, and significantly increased the nuclear localization of Nrf2 in db/db mice (Figure 6A–A'). Analysis of the RNA-Seq data showed a strong upregulation of a set of canonical Nrf2 target genes (Figure 6C), including those with antioxidant functions (*Nqo1, Txn1, Gsr, Gclc, Gstm1*), those involved in iron metabolism (*Ftl1 and Fth1*), and those that produce NADPH (*Me1, G6pdx, Idh1*) [17], while the expression of *Keap1*, a negative regulator of Nrf2 [20], was decreased. In addition, the levels of 8-hydroxydeoxyguanosine (8OHdG), a marker of DNA damage, were significantly decreased in both db/+ and db/db mice after DG-041 treatment (Figure 7A–B). Together, these data demonstrate that EP3 blockade activates the Nrf2 pathway, providing a possible explanation for the sparing of β-cell mass by DG-041.

4. DISCUSSION

The current study reveals that *in vivo* pharmacological blockade of the G_i-coupled PGE_2 receptor EP3 improves the β-cell phenotype in a mouse model of T2D. The major findings are as follows: 1) increase in β-cell proliferation and mass in response to EP3 blockade, with no significant effect on β-cell survival, 2) restoration of islet morphology and improved expression of genes that enhance β-cell identity and function, and 3) activation of the Nrf2 antioxidant pathway.

In our previous *ex vivo* studies with isolated islets, β-cell proliferation in response to EP3 blockade required the presence of an additional proliferative cue (placental lactogen) in mouse islets but not human islets [16]. It is possible that in db/db mice, the chronic inflammatory state and/or β-cell oxidative stress [45,46] contribute to the response

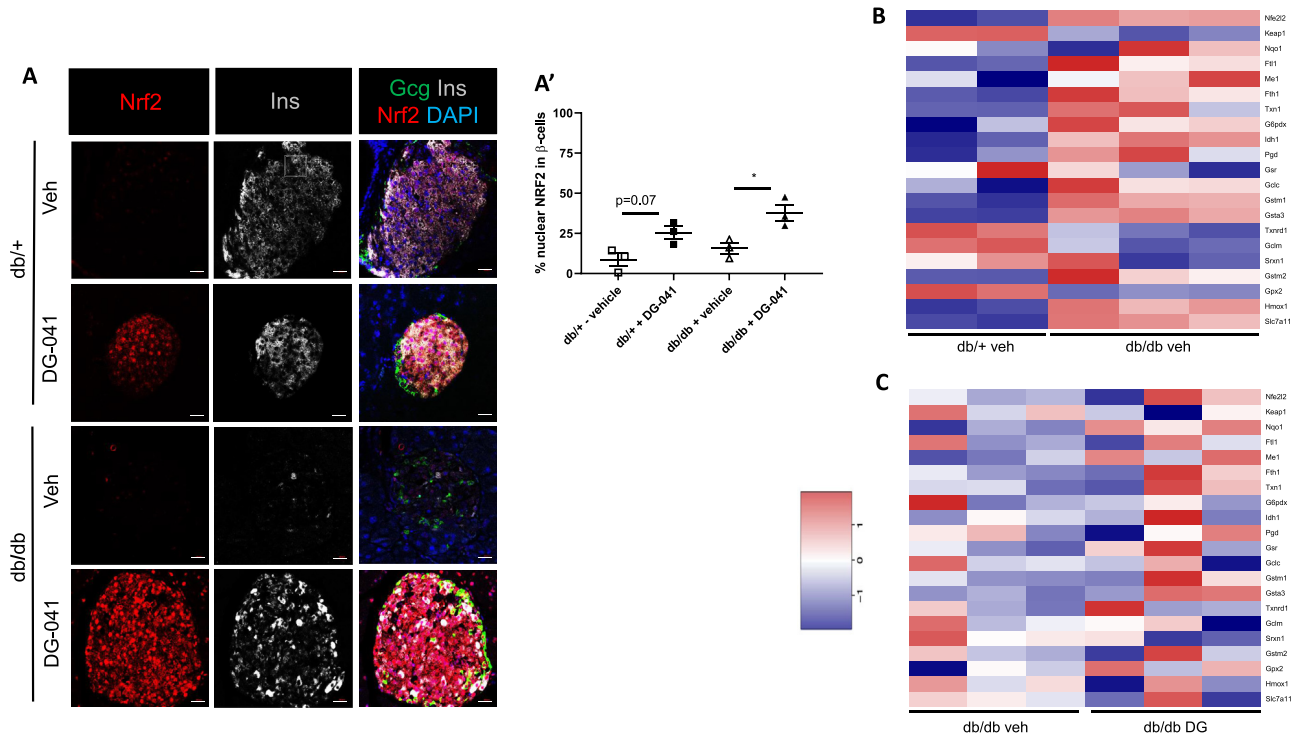

Figure 6: EP3 blockade activates the Nrf2 antioxidant pathway. (A) Paraffin-embedded sections from pancreata isolated from the indicated genotype and treatment groups were immunolabeled with antibodies directed against insulin (Ins; white), glucagon (Gcg; green), or Nrf2 (red). Nuclei were stained with DAPI (blue). Depicted are representative images of three individual mice in each group. (A) Quantification of nuclear Nrf2 in β-cells. One asterisk indicates $p < 0.05$. (B) Heatmap depicting alterations in the expression of *Nrf2(Nfe2l2)* and selected Nrf2 target genes between vehicle-treated db/+ and db/db mice. (C) Heatmap depicting alterations in the expression of *Nrf2(Nfe2l2)* and selected target genes between vehicle-treated and DG-041-treated db/db mice. Mice were treated from 6 to 8 weeks of age. Red indicates high expression; blue indicates low expression. (Scale bar, 20 μm)

to an EP3 antagonist, leading to increased β-cell proliferation. Inflammation-associated PGE_2 production is increased in the setting of T2D [7] and correlates with reduced GSIS [47,48] — an effect that is relieved with EP3 blockade *ex vivo* [7]. Inhibition of PGE_2 production itself has yielded conflicting effects on β-cell function [47], possibly because of the beneficial effects of PGE_2 acting through the EP4 receptor, effects that would be lost by decreasing the PGE_2 ligand [49]. Thus, EP3 antagonism could alleviate the negative effects of PGE_2 on β cells, thereby allowing PGE_2 to signal through EP4 to enhance β-cell function [16,50]. Alternatively, hyperglycemia may act as the additional proliferative cue required for the EP3 antagonist to induce its proliferative effect, since the current studies were performed at a time point when db/db mice already show elevated blood glucose. It is interesting to note that while we observed an increase in proliferation in the 4—6 week age group, we did not see an increase in mass at this time point. This may reflect a delay between the induction of proliferation and a detectable expansion of mass, as reported previously [51]. In addition, the increase in mass despite a lack of proliferation seen in the 6—8 week treatment group may be explained by increased proliferation at an earlier time point in the treatment paradigm that decreases prior to tissue harvesting. Future studies using tissue harvesting at intermediate time points are needed to address these outstanding questions. Modulation of EP3 has been shown to affect β-cell death [16,52—54]. In our study, TUNEL labeling was not significantly altered between db/+ and db/db mice at either time point. However, there was a trend toward increased β-cell death in DG-041-treated db/db mice at six weeks of age and decreased β-cell death at eight weeks of age. This may also modestly contribute to the effects seen on β-cell mass.

A previous analysis of islet gene expression in db/db mice performed at 13 weeks of age, during overt diabetes, revealed significant downregulation of many genes involved in the insulin secretion pathway [55]. Proteomic analysis was performed to characterize the alterations in the signaling pathways in islets from 13-week-old db/db mice, with a particular focus on the GSK3-Pdx1 axis [33]. We observed changes in the expression of a similar subset of genes in db/db islets at eight weeks of age compared with that of db/+ islets and also detected an upregulation of glucagon expression. Many of the gene expression changes were reversed following EP3 blockade. We also found that the expression of 123 genes was altered in db/+ islets upon exposure to the EP3 antagonist. To our surprise, DG-041 treatment led to different sets of DE genes in db/+ versus db/db mice, suggesting that the effect of EP3 blockade on gene expression differs in the setting of hyperglycemia present in db/db mice.

In several mouse models of diabetes, including db/db mice, the characteristic core and mantle architecture of the mouse islet is lost [56], which occurs concomitantly with lower β/α-cell ratios [30,35]. We found that treatment with the EP3 antagonist preserves normal islet architecture and partially restores the β/α-cell ratio. Our RNA-Seq analysis revealed that many genes encoding integrins, ephrin/EPH signaling, and collagens were upregulated in the setting of hyperglycemia but were not changed following EP3 inhibition. In contrast, a number of genes involved in cell adhesion were altered in the setting of

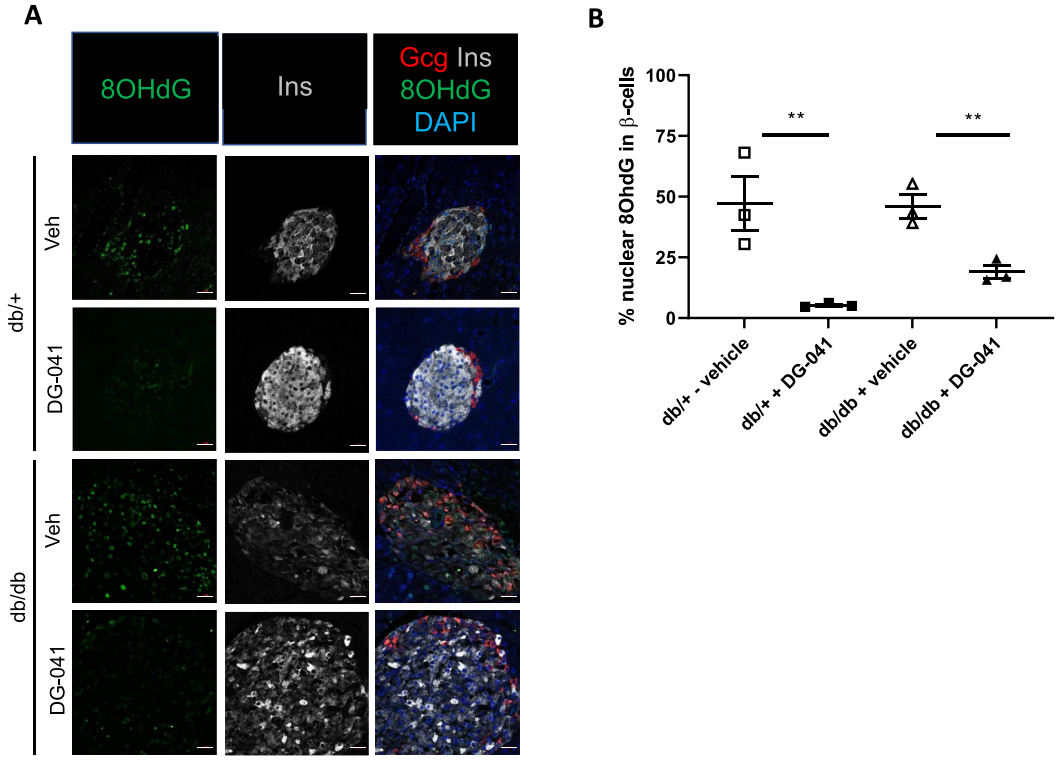

Figure 7: Effects of EP3 blockade on DNA damage in db/+ and db/db mice. (A) Paraffin-embedded sections from pancreata isolated from the indicated genotype and treatment groups were immunolabeled with antibodies directed against insulin (Ins; white), glucagon (Gcg; red), or 8OHdG (green). Nuclei were stained with DAPI (blue). Mice were treated from 6 to 8 weeks of age for 14 days. (Scale bar, 20 μm) (B) Quantification of nuclear 8OHdG in β-cells. Two asterisks indicate $p < 0.01$.

EP3 blockade as well as during hyperglycemia. This suggests that EP3 inhibition either reverses the mixed islet phenotype after it has already been established or attenuates the migration of glucagon+ cells into the core of the islet.

The role of EP3 in modulating β-cell function in mouse and human islets has been postulated [6,7,23,48,49,53,57–59]. Eicosapentaenoic acid-enriched islets display enhanced β-cell function concomitant with reductions in EP3 expression [6]. In contrast, islets obtained from EP3 KO mice do not display differences in GSIS [32]. In the current study, *in vivo* EP3 inhibition did not lead to increased insulin secretion in static incubation assays conducted using isolated islets, nor did it lead to improved glucose tolerance in db/db mice. Potential explanations for these discrepant findings include: 1) EP3 does not regulate β-cell function in db/db mice; 2) the effects of EP3 receptor modulation differ between strains/backgrounds of mice and the underlying metabolic derangements; 3) an inhibitory effect of the increase in *Sst* expression is observed in islets from DG-041-treated db/db mice (although the protein levels were not examined) as has been shown by others [60,61]; 4) longer treatment duration is needed to translate into beneficial effects on glucose homeostasis.

Of particular significance was the induction of gene transcription and nuclear localized protein of Nrf2 in response to EP3 blockade in islets from db/db mice. Nrf2 plays a critical role in counteracting oxidative stress. Under homeostatic conditions, Nrf2 is maintained at low basal levels with a short half-life of approximately 10–30 min; however, under oxidative stress, Nrf2 is stabilized and translocates to the nucleus, where it activates the transcription of target genes in cooperation with the members of the small Maf protein family [17]. Transcriptional targets of Nrf2 include many antioxidant and detoxification enzymes that are integral to the glutathione and thioredoxin antioxidant system, NADPH regeneration, reactive oxygen species (ROS) and xenobiotic detoxification, as well as heme and iron homeostasis [17,62]. Previous studies have shown that Nrf2 suppresses inflammation, improves insulin resistance, and protects β-cells from ROS-induced damage [40,63]. Oxidative stress is increased in diabetic patients as well as in pancreatic islets of *db/db* mice and is associated with impaired regulation of blood glucose [63]. Pancreatic β-cells are unique in that they contain low levels of antioxidant enzymes [64], suggesting that unresolved oxidative stress contributes to the development of diabetes mellitus. Indeed, the transgenic expression of glutathione peroxidase in β-cells of db/db mice reverses diabetes [65]. Transgenic expression of Nrf2 in β-cells leads to increased insulin expression and secretion in iNOS transgenic mice [39], and activation of Nrf2 *via* Keap1 deletion prevents the onset of diabetes in db/db mice [66]. These results strongly suggest that activation of Nrf2 under increased ROS conditions prevents β-cell dedifferentiation and dysfunction [67]. Thus, the restoration of insulin protein and decrease in 8OHdG observed in response to EP3 blockade could be due, in part, to Nrf2 induction. Overexpression of Nrf2 in human islets resulted in an increase in β-cells under both low- and high-glucose conditions, indicating that Nrf2 overexpression is sufficient for human β-cell proliferation [19]. Overall, current evidence suggests that the activation of Nrf2 protects pancreatic β-cells from varying kinds of damage and promotes β-cell proliferation. Thus, elucidating the functional connections between EP3 and Nrf2 are of great translational significance. The mechanisms whereby EP3 blockade leads to increased Nrf2 warrant further investigation.

The current investigation utilizes a model of systemic EP3 blockade. Since EP3 is expressed in α, β, and δ cells [7,68,69], the effects of an

EP3 antagonist on β-cell mass dynamics could be due to the signaling mechanisms elicited *via* EP3 receptor blockade on the other endocrine cells of the pancreas. In addition, the effects observed within the islets could be due to EP3 blockade on other tissues/organs that crosstalk with pancreatic endocrine cells. Therefore, future investigations will include the use of β-cell-specific *Ptger3* inactivation.

5. CONCLUSION

The current study provides evidence that EP3 blockade promotes β-cell mass expansion in a mouse model of T2D. The increase in the GLP-1 receptor expression observed in db/db mice treated with the EP3 antagonist supports the concept that blocking EP3 activity would provide added benefit in the setting of GLP-1 pathway agonist therapy, especially given the lack of efficacy of these treatments in some individuals [70,71].

AUTHOR CONTRIBUTIONS

S.R.A., M.E.K., D.K.S., R.M.B., and M.G. conceived the studies. K.J.B., S.R.A., A.A.S., L.S.K., J.C.D., S.B-A., V.F.R., W.A.P., and D.C.T. performed the experiments. K.J.B., S.R.A., A.A.S., L.S.K., S.B-A., M.A.R., E.M.O., and E.M.W. generated the figures. K.J.B., S.R.A., A.A.S., L.S.K., S.B-A., M.A.R., E.M.O., E.M.W., M.E.K., Q,S., D.K.S., R.M.B., and M.G. analyzed the data. S.R.A. and M.G. wrote the first draft of the manuscript. K.J.B., S.R.A., M.E.K., D.K.S., R.M.B., and M.G. edited and finalized the manuscript.

ACKNOWLEDGEMENTS

We thank the members of the Gannon lab as well as Drs. Alan Attie and Mark Keller (University of Wisconsin, Madison) for their careful reading of the manuscripts and for helpful dicussions. We thank Drs. Xiaodong Zhu and Bethany A Carboneau and Ms. Khushi Patel for their technical assistance. We thank Dr. Mark Huising for giving us access to his laboratory website for use of their open-access comprehensive transcriptomics database. The Islet Procurement and Analysis Core of the Vanderbilt Diabetes Research and Training Center is supported by the National Institutes of Health (Grant DK-20593). S.R.A. was supported in part by the Vanderbilt Integrated Biological Systems Training in Oncology Training Grant (T32CA119925-01A2). A.A.S., E.M.O., and D.T,C. were supported in part by the Vanderbilt University Training Program in Molecular Endocrinology (5T32 DK7563-30). A.A.S. was also supported by an NRSA from NIH/NIDDK (1F31 DK127613-01). M.E.K was funded by NIH award K01 DK102598 and a Merit Review Award from the Department of Veterans Affairs (I01 BX003700). M.G. was supported by a Merit Review Award from the Department of Veterans Affairs (1I01 BX0037440-01) and R01 DK120626. D.K.S. was supported by R01 DK114338. R.M.B. was funded by an R01 HL134895, R21 AG065859, and R03 AG063217. DG-041 was provided by the Vanderbilt Institute of Chemical Biology, Chemical Synthesis Core, Vanderbilt University, Nashville, TN. We would like to thank Dr. Kwangho Kim for his expertise.

CONFLICT OF INTEREST

None declared.

APPENDIX A. SUPPLEMENTARY DATA

Supplementary data to this article can be found online at https://doi.org/10.1016/j.molmet.2021.101347.

REFERENCES

[1] Golson, M.L., Misfeldt, A.A., Kopsombut, U.G., Petersen, C.P., Gannon, M., 2010. High fat diet regulation of β-cell proliferation and β-cell mass. The Open Endocrinology Journal 4:66—77.

[2] Chen, C., Cohrs, C.M., Stertmann, J., Bozsak, R., Speier, S., 2017. Human beta cell mass and function in diabetes: recent advances in knowledge and technologies to understand disease pathogenesis. Molecular Metabolism 6(9):943—957.

[3] Ahren, B., 2009. Islet G protein-coupled receptors as potential targets for treatment of type 2 diabetes. Nature Reviews Drug Discovery 8(5):369—385.

[4] Lavine, J.A., Attie, A.D., 2010. Gastrointestinal hormones and the regulation of beta-cell mass. Annals of the New York Academy of Sciences 1212:41—58.

[5] Anderson, S.L., Trujillo, J.M., McDermott, M., Saseen, J.J., 2012. Determining predictors of response to exenatide in type 2 diabetes. Journal of the American Pharmacists Association (2003) 52(4):466—471.

[6] Neuman, J.C., Schaid, M.D., Brill, A.L., Fenske, R.J., Kibbe, C.R., Fontaine, D.A., et al., 2017. Enriching islet phospholipids with eicosapentaenoic acid reduces prostaglandin E(2) signaling and enhances diabetic β-cell function. Diabetes 66(6):1572—1585.

[7] Kimple, M.E., Keller, M.P., Rabaglia, M.R., Pasker, R.L., Neuman, J.C., Truchan, N.A., et al., 2013. Prostaglandin E2 receptor, EP3, is induced in diabetic islets and negatively regulates glucose- and hormone-stimulated insulin secretion. Diabetes 62(6):1904—1912.

[8] Robertson, R.P., 1988. Eicosanoids as pluripotential modulators of pancreatic islet function. Diabetes 37(4):367—370.

[9] Meng, Z., Lv, J., Luo, Y., Lin, Y., Zhu, Y., Nie, J., et al., 2009. Forkhead box O1/pancreatic and duodenal homeobox 1 intracellular translocation is regulated by c-Jun N-terminal kinase and involved in prostaglandin E2-induced pancreatic beta-cell dysfunction. Endocrinology 150(12):5284—5293.

[10] Meng, Z.X., Sun, J.X., Ling, J.J., Lv, J.H., Zhu, D.Y., Chen, Q., et al., 2006. Prostaglandin E2 regulates Foxo activity via the Akt pathway: implications for pancreatic islet beta cell dysfunction. Diabetologia 49(12):2959—2968.

[11] Robertson, R.P., Tsai, P., Little, S.A., Zhang, H.J., Walseth, T.F., 1987. Receptor-mediated adenylate cyclase-coupled mechanism for PGE2 inhibition of insulin secretion in HIT cells. Diabetes 36(9):1047—1053.

[12] Seaquist, E.R., Walseth, T.F., Nelson, D.M., Robertson, R.P., 1989. Pertussis toxin-sensitive G protein mediation of PGE2 inhibition of cAMP metabolism and phasic glucose-induced insulin secretion in HIT cells. Diabetes 38(11):1439—1445.

[13] Sjoholm, A., 1996. Prostaglandins inhibit pancreatic beta-cell replication and long-term insulin secretion by pertussis toxin-insensitive mechanisms but do not mediate the actions of interleukin-1 beta. Biochimica et Biophysica Acta 1313(2):106—110.

[14] Tran, P.O., Gleason, C.E., Robertson, R.P., 2002. Inhibition of interleukin-1beta-induced COX-2 and EP3 gene expression by sodium salicylate enhances pancreatic islet beta-cell function. Diabetes 51(6):1772—1778.

[15] Oshima, H., Taketo, M.M., Oshima, M., 2006. Destruction of pancreatic beta-cells by transgenic induction of prostaglandin E2 in the islets. Journal of Biological Chemistry 281(39):29330—29336.

[16] Carboneau, B.A., Allan, J.A., Townsend, S.E., Kimple, M.E., Breyer, R.M., Gannon, M., 2017. Opposing effects of prostaglandin E(2) receptors EP3 and EP4 on mouse and human β-cell survival and proliferation. Molecular Metabolism 6(6):548—559.

[17] Tonelli, C., Chio, I.I.C., Tuveson, D.A., 2018. Transcriptional regulation by Nrf2. Antioxidants and Redox Signaling 29(17):1727—1745.

[18] Yagishita, Y., Uruno, A., Fukutomi, T., Saito, R., Saigusa, D., Pi, J., et al., 2017. Nrf2 improves leptin and insulin resistance provoked by hypothalamic oxidative stress. Cell Reports 18(8):2030—2044.

[19] Kumar, A., Katz, L.S., Schulz, A.M., Kim, M., Honig, L.B., Li, L., et al., 2018. Activation of Nrf2 is required for normal and ChREBPα-augmented glucose-stimulated β-cell proliferation. Diabetes 67(8):1561–1575.

[20] Heiss, C.N., Manneras-Holm, L., Lee, Y.S., Serrano-Lobo, J., Hakansson Gladh, A., Seeley, R.J., et al., 2021. The gut microbiota regulates hypothalamic inflammation and leptin sensitivity in Western diet-fed mice via a GLP-1R-dependent mechanism. Cell Reports 35(8):109163.

[21] Ast, J., Arvaniti, A., Fine, N.H.F., Nasteska, D., Ashford, F.B., Stamataki, Z., et al., 2020. Author Correction: super-resolution microscopy compatible fluorescent probes reveal endogenous glucagon-like peptide-1 receptor distribution and dynamics. Nature Communications 11(1):5160.

[22] Elsakr, J.M., Dunn, J.C., Tennant, K., Zhao, S.K., Kroeten, K., Pasek, R.C., et al., 2019. Maternal Western-style diet affects offspring islet composition and function in a non-human primate model of maternal over-nutrition. Molecular Metabolism 25:73–82.

[23] Dadi, P.K., Vierra, N.C., Ustione, A., Piston, D.W., Colbran, R.J., Jacobson, D.A., 2014. Inhibition of pancreatic β-cell Ca2+/calmodulin-dependent protein kinase II reduces glucose-stimulated calcium influx and insulin secretion, impairing glucose tolerance. Journal of Biological Chemistry 289(18):12435–12445.

[24] Martin, M., 2011. Cutadapt removes adapter sequences from high-throughput sequencing reads. EMBnetjournal 17:10–12.

[25] Dobin, A., Davis, C.A., Schlesinger, F., Drenkow, J., Zaleski, C., Jha, S., et al., 2013. STAR: ultrafast universal RNA-seq aligner. Bioinformatics 29(1):15–21.

[26] Liao, Y., Smyth, G.K., Shi, W., 2014. featureCounts: an efficient general purpose program for assigning sequence reads to genomic features. Bioinformatics 30(7):923–930.

[27] Love, M.I., Huber, W., Anders, S., 2014. Moderated estimation of fold change and dispersion for RNA-seq data with DESeq2. Genome Biology 15(12):550.

[28] Zhao, S., Guo, Y., Sheng, Q., Shyr, Y., 2014. Advanced heat map and clustering analysis using heatmap3. BioMed Research International 2014:986048.

[29] Wang, J., Vasaikar, S., Shi, Z., Greer, M., Zhang, B., 2017. WebGestalt 2017: a more comprehensive, powerful, flexible and interactive gene set enrichment analysis toolkit. Nucleic Acids Research 45(W1):W130–W137.

[30] Guo, S., Dai, C., Guo, M., Taylor, B., Harmon, J.S., Sander, M., et al., 2013. Inactivation of specific β cell transcription factors in type 2 diabetes. Journal of Clinical Investigation 123(8):3305–3316.

[31] Ceddia, R.P., Downey, J.D., Morrison, R.D., Kraemer, M.P., Davis, S.E., Wu, J., et al., 2019. The effect of the EP3 antagonist DG-041 on male mice with diet-induced obesity. Prostaglandins & Other Lipid Mediators, 106353.

[32] Ceddia, R.P., Lee, D., Maulis, M.F., Carboneau, B.A., Threadgill, D.W., Poffenberger, G., et al., 2016. The PGE2 EP3 receptor regulates diet-induced adiposity in male mice. Endocrinology 157(1):220–232.

[33] Sacco, F., Seelig, A., Humphrey, S.J., Krahmer, N., Volta, F., Reggio, A., et al., 2019. Phosphoproteomics reveals the GSK3-PDX1 Axis as a key pathogenic signaling node in diabetic islets. Cell Metabolism 29(6):1422–14232 e3.

[34] Lu, A., Zuo, C., He, Y., Chen, G., Piao, L., Zhang, J., et al., 2015. EP3 receptor deficiency attenuates pulmonary hypertension through suppression of Rho/TGF-β1 signaling. Journal of Clinical Investigation 125(3):1228–1242.

[35] Liu, Z., Kim, W., Chen, Z., Shin, Y.K., Carlson, O.D., Fiori, J.L., et al., 2011. Insulin and glucagon regulate pancreatic α-cell proliferation. PLoS One 6(1):e16096.

[36] Petry, S.F., Sun, L.M., Knapp, A., Reinl, S., Linn, T., 2018. Distinct shift in beta-cell glutaredoxin 5 expression is mediated by hypoxia and lipotoxicity both in vivo and in vitro. Frontiers in Endocrinology (Lausanne) 9:84.

[37] Kim, A., Miller, K., Jo, J., Kilimnik, G., Wojcik, P., Hara, M., 2009. Islet architecture: a comparative study. Islets 1(2):129–136.

[38] Adams, M.T., Gilbert, J.M., Hinojosa Paiz, J., Bowman, F.M., Blum, B., 2018. Endocrine cell type sorting and mature architecture in the islets of Langerhans require expression of Roundabout receptors in β cells. Scientific Reports 8(1):10876.

[39] Yagishita, Y., Fukutomi, T., Sugawara, A., Kawamura, H., Takahashi, T., Pi, J., et al., 2014. Nrf2 protects pancreatic beta-cells from oxidative and nitrosative stress in diabetic model mice. Diabetes 63(2):605–618.

[40] Baumel-Alterzon, S., Katz, L.S., Brill, G., Garcia-Ocana, A., Scott, D.K., 2021. Nrf2: the master and captain of beta cell fate. Trends in Endocrinology and Metabolism: TEM 32(1):7–19.

[41] Gong, P., Stewart, D., Hu, B., Li, N., Cook, J., Nel, A., et al., 2002. Activation of the mouse heme oxygenase-1 gene by 15-deoxy-Delta(12,14)-prostaglandin J(2) is mediated by the stress response elements and transcription factor Nrf2. Antioxidants and Redox Signaling 4(2):249–257.

[42] Itoh, K., Mochizuki, M., Ishii, Y., Ishii, T., Shibata, T., Kawamoto, Y., et al., 2004. Transcription factor Nrf2 regulates inflammation by mediating the effect of 15-deoxy-Delta(12,14)-prostaglandin j(2). Molecular and Cellular Biology 24(1):36–45.

[43] Katsumata, Y., Shinmura, K., Sugiura, Y., Tohyama, S., Matsuhashi, T., Ito, H., et al., 2014. Endogenous prostaglandin D2 and its metabolites protect the heart against ischemia-reperfusion injury by activating Nrf2. Hypertension 63(1):80–87.

[44] Fernández-Millán, E., Martín, M.A., Goya, L., Lizárraga-Mollinedo, E., Escrivá, F., Ramos, S., et al., 2016. Glucagon-like peptide-1 improves beta-cell antioxidant capacity via extracellular regulated kinases pathway and Nrf2 translocation. Free Radical Biology and Medicine 95:16–26.

[45] Dalbøge, L.S., Almholt, D.L., Neerup, T.S., Vassiliadis, E., Vrang, N., Pedersen, L., et al., 2013. Characterisation of age-dependent beta cell dynamics in the male db/db mice. PLoS One 8(12):e82813.

[46] Wang, J., Wang, H., 2017. Oxidative stress in pancreatic beta cell regeneration. Oxidation Medicine Cell Longevity 2017:1930261.

[47] Neuman, J.C., Schaid, M.D., Brill, A.L., Fenske, R.J., Kibbe, C.R., Fontaine, D.A., et al., 2017. Enriching islet phospholipids with eicosapentaenoic acid reduces prostaglandin E2 signaling and enhances diabetic beta-cell function. Diabetes 66(6):1572–1585.

[48] Schaid, M.D., Zhu, Y., Richardson, N.E., Patibandla, C., Ong, I.M., Fenske, R.J., et al., 2021. Systemic metabolic alterations correlate with islet-level prostaglandin E2 production and signaling mechanisms that predict beta-cell dysfunction in a mouse model of type 2 diabetes. Metabolites 11(1):58.

[49] Sandhu, H.K., Neuman, J.C., Schaid, M.D., Davis, S.E., Connors, K.M., Challa, R., et al., 2021. Rat prostaglandin EP3 receptor is highly promiscuous and is the sole prostanoid receptor family member that regulates INS-1 (832/3) cell glucose-stimulated insulin secretion. Pharmacological Research Perspect 9(2):e00736.

[50] Carboneau, B.A., Breyer, R.M., Gannon, M., 2017. Regulation of pancreatic β-cell function and mass dynamics by prostaglandin signaling. Journal of Cell Communication Signal 11(2):105–116.

[51] Mosser, R.E., Gannon, M., 2013. An assay for small scale screening of candidate beta cell proliferative factors using intact islets. Biotechniques 55(6):310–312.

[52] Amior, L., Srivastava, R., Nano, R., Bertuzzi, F., Melloul, D., 2019. The role of Cox-2 and prostaglandin E(2) receptor EP3 in pancreatic β-cell death. The FASEB Journal 33(4):4975–4986.

[53] Brill, A.L., Wisinski, J.A., Cadena, M.T., Thompson, M.F., Fenske, R.J., Brar, H.K., et al., 2016. Synergy between galphaz deficiency and GLP-1 analog treatment in preserving functional beta-cell mass in experimental diabetes. Molecular Endocrinology 30(5):543–556.

[54] Fenske, R.J., Cadena, M.T., Harenda, Q.E., Wienkes, H.N., Carbajal, K., Schaid, M.D., et al., 2017. The inhibitory G protein alpha-subunit, galphaz, promotes type 1 diabetes-like pathophysiology in NOD mice. Endocrinology 158(6):1645–1658.

[55] Neelankal John, A., Ram, R., Jiang, F.X., 2018. RNA-seq analysis of islets to characterise the dedifferentiation in type 2 diabetes model mice db/db. Endocrine Pathology 29(3):207–221.

[56] Kim, A., Miller, K., Jo, J., Kilimnik, G., Wojcik, P., Hara, M., 2009. Islet architecture. Islets 1(2):129—136.

[57] Kimple, M.E., Moss, J.B., Brar, H.K., Rosa, T.C., Truchan, N.A., Pasker, R.L., et al., 2012. Deletion of GalphaZ protein protects against diet-induced glucose intolerance via expansion of beta-cell mass. Journal of Biological Chemistry 287(24):20344—20355.

[58] Linnemann, A.K., Neuman, J.C., Battiola, T.J., Wisinski, J.A., Kimple, M.E., Davis, D.B., 2015. Glucagon-like peptide-1 regulates cholecystokinin production in beta-cells to protect from apoptosis. Molecular Endocrinology 29(7):978—987.

[59] Schaid, M.D., Green, C.L., Peter, D.C., Gallagher, S.J., Guthery, E., Carbajal, K.A., et al., 2021. Agonist-independent Galphaz activity negatively regulates beta-cell compensation in a diet-induced obesity model of type 2 diabetes. Journal of Biological Chemistry 296:100056.

[60] Porksen, N., Munn, S.R., Steers, J.L., Veldhuis, J.D., Butler, P.C., 1996. Effects of somatostatin on pulsatile insulin secretion: elective inhibition of insulin burst mass. American Journal of Physiology 270(6 Pt 1):E1043—E1049.

[61] Tirone, T.A., Norman, M.A., Moldovan, S., DeMayo, F.J., Wang, X.P., Brunicardi, F.C., 2003. Pancreatic somatostatin inhibits insulin secretion via SSTR-5 in the isolated perfused mouse pancreas model. Pancreas 26(3):e67—e73.

[62] Chen, Q.M., Maltagliati, A.J., 2018. Nrf2 at the heart of oxidative stress and cardiac protection. Physiological Genomics 50(2):77—97.

[63] Uruno, A., Yagishita, Y., Yamamoto, M., 2015. The Keap1-Nrf2 system and diabetes mellitus. Archives of Biochemistry and Biophysics 566:76—84.

[64] Miki, A., Ricordi, C., Sakuma, Y., Yamamoto, T., Misawa, R., Mita, A., et al., 2018. Divergent antioxidant capacity of human islet cell subsets: a potential cause of beta-cell vulnerability in diabetes and islet transplantation. PLoS One 13(5):e0196570.

[65] Harmon, J.S., Bogdani, M., Parazzoli, S.D., Mak, S.S., Oseid, E.A., Berghmans, M., et al., 2009. β-Cell-specific overexpression of glutathione peroxidase preserves intranuclear MafA and reverses diabetes in db/db mice. Endocrinology 150(11):4855—4862.

[66] Uruno, A., Furusawa, Y., Yagishita, Y., Fukutomi, T., Muramatsu, H., Negishi, T., et al., 2013. The Keap1-Nrf2 system prevents onset of diabetes mellitus. Molecular and Cellular Biology 33(15):2996—3010.

[67] Abebe, T., Mahadevan, J., Bogachus, L., Hahn, S., Black, M., Oseid, E., et al., 2017. Nrf2/antioxidant pathway mediates beta cell self-repair after damage by high-fat diet-induced oxidative stress. JCI Insight 2(24):e92854.

[68] Bramswig, N.C., Everett, L.J., Schug, J., Dorrell, C., Liu, C., Luo, Y., et al., 2013. Epigenomic plasticity enables human pancreatic α to β cell reprogramming. Journal of Clinical Investigation 123(3):1275—1284.

[69] Ku, G.M., Kim, H., Vaughn, I.W., Hangauer, M.J., Myung Oh, C., German, M.S., et al., 2012. Research resource: RNA-Seq reveals unique features of the pancreatic β-cell transcriptome. Molecular Endocrinology 26(10):1783—1792.

[70] Garber, A.J., 2011. Long-acting glucagon-like peptide 1 receptor agonists: a review of their efficacy and tolerability. Diabetes Care 34(Suppl 2):S279—S284.

[71] Shah, M., Vella, A., 2014. Effects of GLP-1 on appetite and weight. Reviews in Endocrine & Metabolic Disorders 15(3):181—187.

